ISSN 1846-6168 (Print), ISSN 1848-5588 (Online)
https://doi.org/10.31803/tg-20180131225708

Preliminary communication

INVESTIGATION OF 3:1 AND 2:1 INTERNAL RESONANCES IN FLUID CONVEYING MICROBEAM

Saim KURAL

Abstract: Microbeams are widely used in micro-electro-mechanical systems (MEMS). These systems are alternatives to piezo-resistive sensors because of their high sensitivity and low power consumption. Unlike with the classical theory of continuous media, in order to see the effects of the system being micro-sized, the effect of micro-structure was added to the system based on the modified couple stress theory (MCST) for fluid conveying microbeam. By using Hamilton's principle, the nonlinear equations of motion for the fluid conveying micro beam were obtained. Microbeam was investigated under electrical field and resting on an elastic foundation. It is assumed that the fluid velocity changes harmonically around a constant velocity and that the electrical field force changes harmonically with time. Approximate solutions of the system were achieved by using the multiple time scale method. 3:1 and 2:1 internal resonance cases were investigated. Detuning parameter-amplitude variation graphs were obtained, and stability areas were shown.

Keywords: fluid conveying micro beam; internal resonance; nonlinear vibration; perturbation methods; stability analysis

1 INTRODUCTION

Micro-electromechanical systems (MEMS), micro-beam-based sensors (MCSs), resonators (a micro-device formed by combining several micro-electro-mechanical systems to produce a vibration of a given frequency, usually at its natural frequency [1]), etc., have been increasingly used in recent years. These systems are attractive alternatives to piezo resistive sensors because of their high sensitivity, low power consumption and low cost. In addition, micro-mechanical systems take up less space and consume less power than large-scale machine systems. With proper serial-production techniques, such systems can be manufactured at very low cost. [2, 3, 4]

Some systems, such as MEMS and MCSs, can convey fluid. It is important to obtain the influence of the fluid and its motion on the microbeam behavior. Today, such fluid-conveying microsystems are widely used for genetic engineering, protein synthesis, micro-chemical and biological analysis, micro-sampling, drug injection, in-situ cooling of microsystems, and microfluidic transport. [5]

Several studies have been reported in the literature about microbeam-based systems. The founder of MEMS is often referred to as the famous physicist Richard Feynman. In 1959, Feynman suggested that very small devices could be produced by vaporizing or accumulating materials [6]. In Feynman's important speech the production of small machines by chemically synthesizing the materials first, then physically bringing them together in atomic order was suggested.

Nowadays, this idea has gone much further and systems in nano-dimensions are trying to be produced. There are studies in the literature about the behavior of these systems; Paidoussis et al. [7] investigated the linear and nonlinear dynamic behaviors of cylindrical beams under water flow. They studied and experimented with the energy transfer by the work-energy principle without solving the equations of motion. Then, Paidoussis et al. [8] studied the 3D dynamics of fluid carrying pipes that have one or several springs supports over their length. They compared the theoretically obtained results with those obtained experimentally. Rinaldi et al. [9] studied the dynamics of microstructures with fluid passing through them. They investigated damping, natural frequency changes and stability states. Kural et al. [10] studied string–beam transition problem and they found an approximate solution by using perturbation methods. Yurddaş et al. [11, 12] investigated nonlinear vibrations of an axially moving string having non-ideal mid-support and multi-support conditions.

The equations obtained in the above studies were based on the classical beam theory (CBT) and they are the same as those obtained in normal dimensions, except for the forces in the nonlinear order. In this case, according to the classical beam theory, there is no difference that the beam is of very small size [13]. However, some research which cannot be explained by the classical beam theory has been observed experimentally. It has been concluded that a microbeam has dimensional effects due to reasons such as impurity, crystal lattice incompatibility, shear stresses and micro cracks. Particularly in the studies carried out, it has been observed that the sliding resistance of the material increases as its dimensions decrease. [14]

Different theories have been produced for microstructures because the classical beam theory cannot explain the size effects. For example, couple stress theory and strain gradient theory. Then, modified couple stress theory (MCST), which is easier to apply, has been proposed by Yang et al. [15]. According to this theory, the tensile tensor is symmetric, and a single material dimension parameter is used. According to other theories, this advantage has been attracting many researchers' interest in the past years. Park and Gao [16] studied the properties of Euler-Bernoulli microbeams with MCST. They have already explained unexplained bending tests for epoxy microbeams. Kong et al. [17] have also investigated boundary value problems for Euler-Bernoulli microbeams

with MCST. They have shown that the new natural frequency values obtained are higher than the classical beam theory. Chen et al. [18] have developed a "Modified Couple Stress" model for bending analysis of first order shear deformation of composite layered beams. Rafiee et al. [19] studied forced oscillations that also observed nonlinear effects for simple-supported microbeams. Ke et al. [20] studied free vibrations for Mindlin microplates using MCST. They show that the size effects are quite large when the thickness of the microplates is close to the material length parameter. Atcı and Bağdatlı studied the effects of non-ideal boundary conditions on the free vibrations of fluid conveying clamped microbeams [21]. They also investigated non-ideal boundary conditions for nonlinear fluid conveying microbeams [22]. Dai et al. [23] studied nonlinear dynamic responses of microcantilevers containing internal fluid flow. They found that with the increase in flow velocity, flutter instability, pull-in instability and the combination of both can occur in this dynamical system. Nikkhah-Bahrami et al. investigated nonlinear vibrations of micropipes conveying fluid [24] and nonlinear stability of fluid-conveying imperfect micropipes [25]. Hadi Arvin presented the flap wise bending free vibration analysis of isotropic rotating Timoshenko microbeams, including the size effects [26]. Lotfi et al. [27] investigated transient behavior and dynamic pull-in instability of electrostatically-actuated fluid-conveying microbeams. Kural et al. [13] investigated nonlinear free vibration of a fixed-fixed microbeam conveying fluid resting on elastic foundation.

In this study, it is assumed that the microbeam is affected by the electrical field force and is on an elastic ground, as shown in Fig. 1. The terms originating from extensions during vibration, elastic ground, damping and electrical field strength have added an additional nonlinear property to the equations of motion. Obtained mathematical model became independent from geometry and material by making the equations of motion dimensionless. It is assumed that the fluid velocity changes harmonically around a constant velocity and the electrical field force changes harmonically with time. Under these conditions, the first two natural frequencies of the system were obtained. The resonance states of 3:1 and 2:1 are examined according to the closeness of these natural frequencies. Amplitude changes for the cases where natural frequency values will form 2:1 and 3:1 internal resonance are obtained and shown in the graphs.

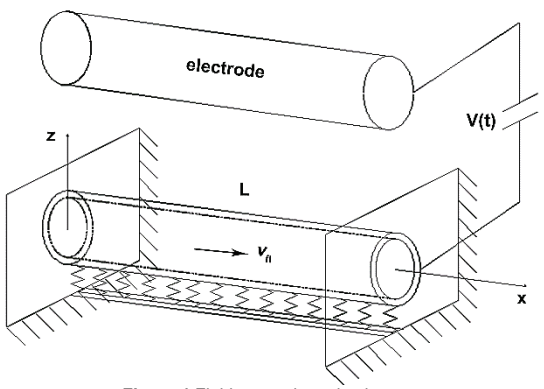

Figure 1 Fluid conveying microbeam

2 LINEAR SOLUTIONS

The equations of motion for the system discussed in this study, in Fig. 1, can be modelled as follows, [28]

$$\begin{aligned}&\ddot{w}+\beta(2v_{fl}\dot{w}'+\dot{v}_{fl}w')+(\beta{v_{fl}}^2-1)w''\\&+({V_f}^2+\Gamma^2)w^{iv}+k_1w+\varepsilon k_2w^3+\varepsilon\bar{\mu}\dot{w}\\&=\varepsilon\bar{\alpha}_2[\frac{1}{2}\int_0^1 w'^2\mathrm{d}x]w''+\varepsilon\bar{\alpha}_1V_{el}(t)^2(1+2w)\end{aligned}\tag{1}$$

Here v_{fl} is fluid velocity, β is solidity ratio, V_f is beam coefficient, Γ is microbeam coefficient, k_1 is linear spring constant, k_2 is nonlinear spring constant, μ is the damping ratio and can be accepted as $O(\varepsilon)$ ($\mu=\varepsilon\bar{\mu}$), $\bar{\alpha}_2$ is the beam elasticity coefficient. For the multiple scale method, the derivatives can be defined as,

$$T_0=t,\quad T_1=\varepsilon t\tag{2}$$

$$\frac{\partial}{\partial t}=\frac{\partial}{\partial T_0}\frac{\partial T_0}{\partial t}+\frac{\partial}{\partial T_1}\frac{\partial T_1}{\partial t}=D_0+\varepsilon D_1+\ldots\tag{3}$$

$$\frac{\partial^2}{\partial t^2}={D_0}^2+2\varepsilon D_0D_1+\ldots\tag{4}$$

We can expand "w" expression as,

$$w=w_0+\varepsilon w_1+\ldots\tag{5}$$

Then the fluid velocity and the electric voltage can be defined,

$$v_{fl}=v_0+\varepsilon v_1\sin\Omega_1t\tag{6}$$

$$V_{el}(t)=V_{AC}\cos\Omega_2t\tag{7}$$

From here, Eq. (1) becomes,

$$\begin{aligned}&({D_0}^2+2\varepsilon D_0D_1)(w_0+\varepsilon w_1)\\&+\beta(2(v_0+\varepsilon v_1\sin\Omega_1T_0)[D_0+\varepsilon D_1](w_0'+\varepsilon w_1')\\&+(\varepsilon v_1\Omega_1\cos\Omega_1T_0)(w_0'+\varepsilon w_1'))\\&+(\beta({v_0}^2+2\varepsilon v_0v_1\sin\Omega_1T_0)-1)(w_0''+\varepsilon w_1'')\\&+({V_f}^2+\Gamma^2)(w_0^{iv}+\varepsilon w_1^{iv})+k_1(w_0+\varepsilon w_1)\\&+\varepsilon k_2(w_0+\varepsilon w_1)+\varepsilon\bar{\mu}[D_0+\varepsilon D_1](w_0+\varepsilon w_1)\\&=\varepsilon\bar{\alpha}_2[\frac{1}{2}\int_0^1({w_0'}^2+2\varepsilon w_0'w_1'+\varepsilon^2{w_1'}^2)\mathrm{d}x](w_0''+\varepsilon w_1'')\\&+\varepsilon\bar{\alpha}_1{V_{AC}}^2\cos^2\Omega_2t(1+2w_0+3{w_0}^2)\end{aligned}\tag{8}$$

If the expression is separated into ranks, Order (1) and Order (ε) are obtained as follows,

$$\underline{O(1)}$$

$$D_0{}^2 w_0 + 2\beta v_0 D_0 w_0{}' + (\beta v_0{}^2 - 1) w_0{}'' + (V_f{}^2 + \Gamma^2) w_0{}^{iv} + k_1 w_0 = 0 \tag{9}$$

$$\underline{O(\varepsilon)}$$

$$\begin{aligned} &D_0{}^2 w_1 + 2\beta v_0 D_0 w_1{}' + (\beta v_0{}^2 - 1) w_1{}'' \\ &+ (V_f{}^2 + \Gamma^2) w_1{}^{iv} + k_1 w_1 = -2 D_0 D_1 w_0 \\ &-2\beta v_0 D_1 w_0{}' - 2 v_1 \sin\Omega_1 T_0 D_0 w_0{}' \\ &-\beta v_1 \Omega_1 \cos\Omega_1 T_0 w_0{}' - 2\beta v_0 v_1 \sin\Omega_1 T_0 D_0 w_0{}'' \\ &-k_2 w_0 - \bar{\mu} D_0 w_0 + \bar{\alpha}_2 (\frac{1}{2}\int_0^1 w_0{}'^2 \mathrm{d}x) w_0{}'' \\ &+ \bar{\alpha}_1 V_{AC}{}^2 \cos^2\Omega_2 T_0 (1 + 2 w_0) \end{aligned} \tag{10}$$

The first order solution can be written as the sum of the infinite number of modes,

$$w_0(x, T_0, T_1) = \sum_{m=0}^{\infty} Y_m(x) A_m(T_1) e^{i\omega_m T_0} + K.E. \tag{11}$$

This solution can be written in linear order as,

$$\begin{aligned} &(V_f{}^2 + \Gamma^2) Y_m{}^{iv} + (\beta v_0{}^2 - 1) Y_m{}'' + 2 i \omega_m \beta v_0 Y_m{}' \\ &+ (k_1 - \omega_m{}^2) Y_m = 0 \end{aligned} \tag{12}$$

Here $Y_m(x)$ solution is offered as,

$$\begin{aligned} Y_m(x) &= c_{m1} e^{i r_{m1} x} + c_{m2} e^{i r_{m2} x} + c_{m3} e^{i r_{m3} x} + c_{m4} e^{i r_{m4} x} \\ &= c_{m1} (e^{i r_{m1} x} + \frac{c_{m2}}{c_{m1}} e^{i r_{m2} x} + \frac{c_{m3}}{c_{m1}} e^{i r_{m3} x} + \frac{c_{m4}}{c_{m1}} e^{i r_{m4} x}) \end{aligned} \tag{13}$$

We can change the coefficients in this equation as follows,

$$\frac{c_{m2}}{c_{m1}} = C_{m2}, \quad \frac{c_{m3}}{c_{m1}} = C_{m3}, \quad \frac{c_{m4}}{c_{m1}} = C_{m4} \tag{14}$$

Hence,

$$\begin{aligned} &c_{m1}\{e^{i r_{m1} x} (r_{m1}{}^4 (V_f{}^2 + \Gamma^2) - r_{m1}{}^2 (\beta v_0{}^2 - 1) \\ &- r_{m1} 2\omega_m \beta v_0 + (k_1 - \omega_m{}^2)) + C_{m2} e^{i r_{m2} x} (r_{m2}{}^4 (V_f{}^2 + \Gamma^2) \\ &- r_{m2}{}^2 (\beta v_0{}^2 - 1) - r_{m2} 2\omega_m \beta v_0 + (k_1 - \omega_m{}^2)) \\ &+ C_{m3} e^{i r_{m3} x} (r_{m3}{}^4 (V_f{}^2 + \Gamma^2) - r_{m3}{}^2 (\beta v_0{}^2 - 1) \\ &- r_{m3} 2\omega_m \beta v_0 + (k_1 - \omega_m{}^2)) + C_{m4} e^{i r_{m4} x} (r_{m4}{}^4 (V_f{}^2 + \Gamma^2) \\ &- r_{m4}{}^2 (\beta v_0{}^2 - 1) - r_{m4} 2\omega_m \beta v_0 + (k_1 - \omega_m{}^2))\} = 0 \end{aligned} \tag{15}$$

In Eq. (15) coefficients cannot be zero; the inside of the parentheses must be zero. For this,

$$\begin{aligned} &r_{mn}{}^4 (V_f{}^2 + \Gamma^2) - r_{mn}{}^2 (\beta v_0{}^2 - 1) \\ &- r_{mn} 2\omega_m \beta v_0 + (k_1 - \omega_m{}^2) = 0 \qquad n = 1, 2, 3, 4 \end{aligned} \tag{16}$$

If we apply the boundary conditions, then the solution of the linear order becomes,

$$\begin{aligned} Y_{mn}(x) = c_{1mn} (& e^{i r_{1mn} x} - \frac{(r_{4mn} - r_{1mn})(e^{i r_{3mn}} - e^{i r_{2mn}})}{(r_{4mn} - r_{2mn})(e^{i r_{3mn}} - e^{i r_{2mn}})} e^{i r_{2mn} x} \\ & - \frac{(r_{4mn} - r_{1mn})(e^{i r_{1mn}} - e^{i r_{2mn}})}{(r_{4mn} - r_{3mn})(e^{i r_{3mn}} - e^{i r_{2mn}})} e^{i r_{3mn} x} \\ & + \frac{\begin{pmatrix} -(r_{4mn} - r_{2mn})(r_{4mn} - r_{3mn})(e^{i r_{3mn}} - e^{i r_{2mn}}) \\ +(r_{4mn} - r_{3mn})(r_{4mn} - r_{1mn})(e^{i r_{3mn}} - e^{i r_{1mn}}) \\ +(r_{4mn} - r_{2mn})(r_{4mn} - r_{1mn})(e^{i r_{1mn}} - e^{i r_{2mn}}) \end{pmatrix}}{(r_{4mn} - r_{2mn})(r_{4mn} - r_{3mn})(e^{i r_{3mn}} - e^{i r_{2mn}})}) = 0 \end{aligned} \tag{17}$$

The C coefficients are determined to provide the following equation.

$$\int_0^1 Y_m{}^2 \mathrm{d}x = 1 \tag{18}$$

With this solution, if the first two natural frequencies of the system will be displayed in tabular form for different conditions as follows,

Table 1 Case 1 - first two natural frequencies of system for fluid velocity changes ($V_f = 1, k_1 = 1, k_2 = 1, v_1 = 3, \varepsilon = 0.1, \beta = 0.5, \alpha_2 = 3$)

v_0	ω_1	ω_2	ω_2 / ω_1
4.300	22.708	67.486	2.972
4.350	22.637	67.421	2.978
4.400	22.566	67.354	2.985
4.450	22.493	67.287	2.991
4.500	22.420	67.219	2.998
4.550*	22.345*	67.150*	3.005*
4.600	22.270	67.080	3.012
4.650	22.193	67.009	3.019
4.700	22.116	66.938	3.027

Table 2 Case 2 - first two natural frequencies of system for fluid velocity changes ($V_f = 0.8, k_1 = 1, k_2 = 1, v_1 = 3, \varepsilon = 0.1, \beta = 0.5, \alpha_2 = 3$)

v_0	ω_1	ω_2	ω_2 / ω_1
3.500	18.210	54.063	2.969
3.550	18.138	53.996	2.977
3.600	18.065	53.929	2.985
3.650	17.991	53.860	2.994
3.700*	17.916*	53.790*	3.002*
3.750	17.839	53.719	3.011
3.800	17.761	53.647	3.020
3.850	17.682	53.574	3.030
3.900	17.602	53.500	3.039

As can be seen from the graphs, the 3:1 internal resonance is a more common problem in the studied situations, while the 2:1 internal resonance condition occurs

when the spring constant is higher. From these graphs nonlinear problem is analyzed, stability limits are plotted by using * values (critical values for internal resonance).

Table 3 Case 3 - first two natural frequencies of system for fluid velocity changes ($V_f = 0.1, k_1 = 1, k_2 = 1, v_1 = 3, \varepsilon = 0.1, \beta = 0.5, \alpha_2 = 3$)

v_0	ω_1	ω_2	ω_2/ω_1
1.150	3.027	8.032	2.653
1.200	2.893	7.873	2.722
1.250	2.750	7.706	2.802
1.300	2.598	7.531	2.899
1.350*	2.437*	7.348*	3.015*
1.400	2.265	7.157	3.160
1.450	2.081	6.956	3.342
1.500	1.885	6.746	3.579
1.550	1.673	6.527	3.901

Table 4 Case 4 - first two natural frequencies of system for fluid velocity changes ($V_f = 0.1, k_1 = 8, k_2 = 1, v_1 = 3, \varepsilon = 0.1, \beta = 0.5, \alpha_2 = 3$)

v_0	ω_1	ω_2	ω_2/ω_1
0.300	5.048	10.004	1.982
0.350	5.019	9.964	1.985
0.400	4.984	9.917	1.990
0.450	4.945	9.864	1.995
0.500*	4.901*	9.805*	2.001*
0.550	4.852	9.739	2.007
0.600	4.798	9.668	2.015
0.650	4.739	9.589	2.024
0.700	4.675	9.505	2.033

3 NONLINEAR PROBLEM AND INTERNAL RESONANCES

Examination of internal resonance states will form nonlinear order solutions. In this section, the effects of nonlinear expressions on the system will be investigated. We define the first order solution as the sum of only the first two modes as follows,

$$w_0(x,T_0,T_1) = A_1(T_1)e^{i\omega_1 T_0}Y_1(x) + A_2(T_1)e^{i\omega_2 T_0}Y_2(x) + K.E. \tag{19}$$

In this case the nonlinear order expression becomes,

$$\begin{aligned} &D_0{}^2 w_1 + 2\beta v_0 D_0 w_1{}' + (\beta v_0{}^2 - 1)w_1{}'' \\ &+(V_f{}^2 + \Gamma^2)w_1{}^{iv} + k_1 w_1 = -2D_0 D_1 w_0 - 2\beta v_0 D_1 w_0{}' \\ &-2\beta v_1 \sin\Omega_1 T_0 D_0 w_0{}' - \beta v_1 \Omega_1 \cos\Omega_1 T_0 w_0{}' \\ &-2\beta v_0 v_1 \sin\Omega_1 T_0 D_0 w_0{}'' - k_2 w_0^3 - \bar{\mu} D_0 w_0 \\ &+\bar{\alpha}_2 (\frac{1}{2}\int_0^1 w_0{}'^2 dx) w_0{}'' + F\cos^2\Omega_2 T_0 (1 + 2w_0) \end{aligned} \tag{20}$$

For simplicity, the force amplitude can be defined as follows,

$$F = \bar{\alpha}_1 V_{AC}{}^2 \tag{21}$$

we can suggest the solution of the nonlinear order as follows,

$$\begin{aligned} &w_1(x,T_0,T_1;\varepsilon) = \phi_1(x,T_1)e^{i\omega_1 T_0} + \phi_2(x,T_1)e^{i\omega_2 T_0} \\ &+W(x,T_0,T_1) + K.E. \end{aligned} \tag{22}$$

we obtain following equation if we write trigonometric expressions in complex form and write all expressions.

$$\begin{aligned} &(V_f{}^2 + \Gamma^2)w_1{}^{iv} + (\beta v_0{}^2 - 1)w_1{}'' + 2\beta v_0 D_0 w_1{}' + D_0{}^2 w_1 + k_1 w_1 \\ &= -2(i\omega_1 Y_1 + \beta v_0 Y_1{}')D_1 A_1 e^{i\omega_1 T_0} - 2(i\omega_2 Y_2 + \beta v_0 Y_2{}')D_1 A_2 e^{i\omega_2 T_0} \\ &-\beta v_1 \omega_1 Y_1{}' A_1 e^{i\omega_2 T_0} e^{i(\sigma_2 - \sigma_1)T_1} + \beta v_1 \omega_1 \overline{Y}_1{}' \overline{A}_1 e^{i\omega_1 T_0} e^{i\sigma_2 T_1} \\ &+\beta v_1 \omega_2 Y_2{}' A_2 e^{i\omega_1 T_0} e^{i(\sigma_1 - \sigma_2)T_1} - \frac{1}{2}\beta v_1 \Omega_1 Y_1{}' A_1 e^{i\omega_2 T_0} e^{i(\sigma_2 - \sigma_1)T_1} \\ &-\frac{1}{2}\beta v_1 \Omega_1 \overline{Y}_1{}' \overline{A}_1 e^{i\omega_1 T_0} e^{i\sigma_2 T_1} - \frac{1}{2}\beta v_1 \Omega_1 Y_2{}' A_2 e^{i\omega_1 T_0} e^{i(\sigma_1 - \sigma_2)T_1} \\ &+i\beta v_0 v_1 Y_1{}'' A_1 e^{i\omega_2 T_0} e^{i(\sigma_2 - \sigma_1)T_1} + i\beta v_0 v_1 \overline{Y}_1{}'' \overline{A}_1 e^{i\omega_1 T_0} e^{i\sigma_2 T_1} \\ &-i\beta v_0 v_1 Y_2{}'' A_2 e^{i\omega_1 T_0} e^{i(\sigma_1 - \sigma_2)T_1} - k_2 (A_1{}^3 Y_1{}^3 e^{i\omega_2 T_0} e^{-i\sigma_1 T_1} \\ &+3A_1{}^2 \overline{A}_1 Y_1{}^2 \overline{Y}_1 e^{i\omega_1 T_0} + 3A_2{}^2 \overline{A}_2 Y_2{}^2 \overline{Y}_2 e^{i\omega_2 T_0} \\ &+3\overline{A}_1{}^2 A_2 \overline{Y}_1{}^2 Y_2 e^{i\omega_1 T_0} e^{i\sigma_1 T_1} + 6A_1 A_2 \overline{A}_1 Y_1 Y_2 \overline{Y}_1 e^{i\omega_2 T_0} \\ &+6A_1 A_2 \overline{A}_2 Y_1 Y_2 \overline{Y}_2 e^{i\omega_1 T_0}) - \bar{\mu}(i\omega_1 A_1 Y_1 e^{i\omega_1 T_0} + i\omega_2 A_2 Y_2 e^{i\omega_2 T_0}) \\ &+\frac{\bar{\alpha}_2}{2}(e^{i\omega_1 T_0}(A_1{}^2 \overline{A}_1 \overline{Y}_1{}'' \int_0^1 Y_1{}'^2 dx + 2A_1 A_2 \overline{A}_2 \overline{Y}_2{}'' \int_0^1 Y_1{}' Y_2{}' dx \\ &+2A_1{}^2 \overline{A}_1 Y_1{}'' \int_0^1 Y_1{}' \overline{Y}_1{}' dx + 2A_1 A_2 \overline{A}_2 Y_2{}'' \int_0^1 Y_1{}' \overline{Y}_2{}' dx \\ &+2A_1 A_2 \overline{A}_2 Y_1{}'' \int_0^1 Y_2{}' \overline{Y}_2{}' dx) + e^{i\omega_2 T_0}(A_2{}^2 \overline{A}_2 \overline{Y}_2{}'' \int_0^1 Y_2{}'^2 dx \\ &+2A_1 A_2 \overline{A}_1 \overline{Y}_1{}'' \int_0^1 Y_1{}' Y_2{}' dx + 2A_2{}^2 \overline{A}_2 Y_2{}'' \int_0^1 Y_2{}' \overline{Y}_2{}' dx \\ &+2A_1 A_2 \overline{A}_1 Y_1{}'' \int_0^1 \overline{Y}_1{}' Y_2{}' dx + 2A_1 A_2 \overline{A}_1 Y_2{}'' \int_0^1 Y_1{}' \overline{Y}_1{}' dx)) \\ &+F(A_1 Y_1 e^{i\omega_1 T_0} + A_2 Y_2 e^{i\omega_2 T_0}) + K.E. + S.O.T. \end{aligned} \tag{23}$$

Here we need a state of solvency to eliminate the concepts that make secularism. We will examine the resolvability conditions in separate sections for different states of internal resonances.

3.1 The Case Where the Fundamental Parametric Resonance and the 3:1 Internal Resonance Conditions are Together

In this case, the fluid velocity change frequency is taken as the critical forcing frequency. The frequency of the electric voltage change was chosen so as not to create any secularity.

$$\begin{aligned} &\omega_2 = 3\omega_1 + \varepsilon\sigma_1 \\ &\Omega_1 = 2\omega_1 + \varepsilon\sigma_2 \\ &\Omega_2 \not\approx 0, \omega_1, 2\omega_1 \end{aligned} \tag{24}$$

Since the homogeneous equation has non-simple solutions, the nonhomogeneous equation can only accept

solutions with a solvability condition. Hence, the following conditions must be met for secularity-forming terms,

$$\begin{aligned}
&\int_0^1[-2(i\omega_1 Y_1+\beta v_0 Y_1')D_1A_1+\beta v_1\omega_1\overline{Y}_1'\overline{A}_1e^{i\sigma_2T_1}\\
&+\beta v_1\omega_2 Y_2'A_2e^{i(\sigma_1-\sigma_2)T_1}-\frac{1}{2}\beta v_1\Omega_1\overline{Y}_1'\overline{A}_1e^{i\sigma_2T_1}\\
&-\frac{1}{2}\beta v_1\Omega_1 Y_2'A_2e^{i(\sigma_1-\sigma_2)T_1}+i\beta v_0v_1\overline{Y}_1''\overline{A}_1e^{i\sigma_2T_1}\\
&-i\beta v_0v_1Y_2''A_2e^{i(\sigma_1-\sigma_2)T_1}-k_2(3A_1^2\overline{A}_1Y_1^2\overline{Y}_1\\
&+3\overline{A}_1^2A_2\overline{Y}_1^2Y_2e^{i\sigma_1T_1}+6A_1A_2\overline{A}_2Y_1Y_2\overline{Y}_2)-\overline{\mu}\,\mathrm{i}\,\omega_1A_1Y_1\\
&+\frac{\overline{\alpha}_2}{2}(A_1^2\overline{A}_1\overline{Y}_1''\int_0^1Y_1'^2\mathrm{d}x+2A_1A_2\overline{A}_2\overline{Y}_2''\int_0^1Y_1'Y_2'\mathrm{d}x\\
&+2A_1^2\overline{A}_1Y_1''\int_0^1Y_1'\overline{Y}_1'\mathrm{d}x+2A_1A_2\overline{A}_2Y_2''\int_0^1Y_1'\overline{Y}_2'\mathrm{d}x\\
&+2A_1A_2\overline{A}_2Y_1''\int_0^1Y_2'\overline{Y}_2'\mathrm{d}x)+\mathrm{F}\,A_1Y_1]\overline{Y}_1\mathrm{d}x=0
\end{aligned}\tag{25}$$

$$\begin{aligned}
&\int_0^1[-2(i\omega_2Y_2+\beta v_0Y_2')D_1A_2-\beta v_1\omega_1Y_1'A_1e^{i(\sigma_2-\sigma_1)T_1}\\
&-\frac{1}{2}\beta v_1\Omega_1Y_1'A_1e^{i(\sigma_2-\sigma_1)T_1}+i\beta v_0v_1Y_1''A_1e^{i(\sigma_2-\sigma_1)T_1}\\
&-k_2(A_1^3Y_1^3e^{-i\sigma_1T_1}+3A_2^2\overline{A}_2Y_2^2\overline{Y}_2+6A_1A_2\overline{A}_1Y_1Y_2\overline{Y}_1)\\
&-\overline{\mu}\,\mathrm{i}\,\omega_2A_2Y_2+\frac{\overline{\alpha}_2}{2}(A_2^2\overline{A}_2\overline{Y}_2''\int_0^1Y_2'^2\mathrm{d}x\\
&+2A_1A_2\overline{A}_1\overline{Y}_1''\int_0^1Y_1'Y_2'\mathrm{d}x+2A_2^2\overline{A}_2Y_2''\int_0^1Y_2'\overline{Y}_2'\mathrm{d}x\\
&+2A_1A_2\overline{A}_1Y_1''\int_0^1\overline{Y}_1'Y_2'dx+2A_1A_2\overline{A}_1Y_2''\int_0^1Y_1'\overline{Y}_1'dx)\\
&+FA_2Y_2]\overline{Y}_2\mathrm{d}x=0
\end{aligned}\tag{26}$$

From here, the simplest form of our equations is obtained as follows,

$$\begin{aligned}
&D_1A_1+\overline{A}_1e^{i\sigma_2T_1}K_{11}+A_2e^{i(\sigma_1-\sigma_2)T_1}K_{12}-\overline{A}_1^2A_2e^{i\sigma_1T_1}K_{13}\\
&+A_1K_{14}+A_1^2\overline{A}_1K_{15}+A_1A_2\overline{A}_2K_{16}=0
\end{aligned}\tag{27}$$

$$\begin{aligned}
&D_1A_2-A_1e^{i(\sigma_2-\sigma_1)T_1}K_{21}+A_1^3e^{-i\sigma_1T_1}K_{22}+A_2^2\overline{A}_2K_{23}\\
&+A_2K_{24}+A_1A_2\overline{A}_1K_{25}=0
\end{aligned}\tag{28}$$

The K expressions in the equations defined as follows,

$$\begin{aligned}
K_{11}&=\frac{[(\beta v_1\omega_1-\frac{1}{2}\beta v_1\Omega_1)\int_0^1\overline{Y}_1'\overline{Y}_1\,\mathrm{d}x+i\beta v_0v_1\int_0^1\overline{Y}''\overline{Y}_1\,\mathrm{d}x]}{(-2i\omega_1\int_0^1Y_1\overline{Y}_1\,\mathrm{d}x-2\beta v_0\int_0^1Y_1'\overline{Y}_1\,\mathrm{d}x)},\\
K_{12}&=\frac{[(\beta v_1\omega_2-\frac{1}{2}\beta v_1\Omega_1)\int_0^1Y_2'\overline{Y}_1\,\mathrm{d}x-i\beta v_0v_1\int_0^1Y_2''\overline{Y}_1\,\mathrm{d}x]}{(-2i\omega_1\int_0^1Y_1\overline{Y}_1\,\mathrm{d}x-2\beta v_0\int_0^1Y_1'\overline{Y}_1\,\mathrm{d}x)},\\
K_{13}&=\frac{(3k_2\int_0^1\overline{Y}_1^3Y_2\,\mathrm{d}x)}{(-2i\omega_1\int_0^1Y_1\overline{Y}_1\,\mathrm{d}x-2\beta v_0\int_0^1Y_1'\overline{Y}_1\,\mathrm{d}x)},\\
K_{14}&=\frac{[(-\overline{\mu}\,\mathrm{i}\,\omega_1+\mathrm{F})\int_0^1Y_1\overline{Y}_1\,\mathrm{d}x]}{(-2i\omega_1\int_0^1Y_1\overline{Y}_1\,\mathrm{d}x-2\beta v_0\int_0^1Y_1'\overline{Y}_1\,\mathrm{d}x)},\\
K_{15}&=[-3k_2\int_0^1Y_1^2\overline{Y}_1^2\,\mathrm{d}x+\overline{\alpha}_2(\frac{1}{2}\int_0^1\overline{Y}_1\overline{Y}_1''\int_0^1Y_1'^2dxdx\\
&+\int_0^1\overline{Y}_1Y_1''\int_0^1Y_1'\overline{Y}_1'dxdx)]/(-2i\omega_1\int_0^1Y_1\overline{Y}_1\,\mathrm{d}x-2\beta v_0\int_0^1Y_1'\overline{Y}_1\,\mathrm{d}x),\\
K_{16}&=[-6k_2\int_0^1Y_1\overline{Y}_1Y_2\overline{Y}_2\,\mathrm{d}x+\overline{\alpha}_2(\int_0^1\overline{Y}_1\overline{Y}_2''\int_0^1Y_1'Y_2'dxdx\\
&+\int_0^1\overline{Y}_1Y_2''\int_0^1Y_1'\overline{Y}_2'dxdx\\
&+\int_0^1\overline{Y}_1Y_1''\int_0^1Y_2'\overline{Y}_2'dxdx)]/(-2i\omega_1\int_0^1Y_1\overline{Y}_1\,\mathrm{d}x-2\beta v_0\int_0^1Y_1'\overline{Y}_1\,\mathrm{d}x)
\end{aligned}\tag{29}$$

$$\begin{aligned}
K_{21}&=\frac{[(\beta v_1\omega_1+\frac{1}{2}\beta v_1\Omega_1)\int_0^1\overline{Y}_2Y_1'\mathrm{d}x-i\beta v_0v_1\int_0^1\overline{Y}_2Y_1''\mathrm{d}x]}{(-2i\omega_2\int_0^1Y_2\overline{Y}_2\mathrm{d}x-2\beta v_0\int_0^1\overline{Y}_2Y_2'\mathrm{d}x)},\\
K_{22}&=\frac{(-k_2\int_0^1Y_1^3\overline{Y}_2\mathrm{d}x)}{(-2i\omega_2\int_0^1Y_2\overline{Y}_2\mathrm{d}x-2\beta v_0\int_0^1\overline{Y}_2Y_2'\mathrm{d}x)},\\
K_{23}&=[-3k_2\int_0^1Y_2^2\overline{Y}_2^2\mathrm{d}x+\overline{\alpha}_2(\frac{1}{2}\int_0^1\overline{Y}_2\overline{Y}_2''\int_0^1Y_2'^2\mathrm{d}x\mathrm{d}x\\
&+\int_0^1\overline{Y}_2Y_2''\int_0^1Y_2'\overline{Y}_2'\mathrm{d}x\mathrm{d}x)]/(-2i\omega_2\int_0^1Y_2\overline{Y}_2\mathrm{d}x-2\beta v_0\int_0^1\overline{Y}_2Y_2'\mathrm{d}x),\\
K_{24}&=\frac{[(-\overline{\mu}\,\mathrm{i}\,\omega_2+\mathrm{F})\int_0^1Y_2\overline{Y}_2\mathrm{d}x]}{(-2i\omega_2\int_0^1Y_2\overline{Y}_2\mathrm{d}x-2\beta v_0\int_0^1\overline{Y}_2Y_2'\mathrm{d}x)},\\
K_{25}&=[-6k_2\int_0^1Y_1Y_2\overline{Y}_1\overline{Y}_2\mathrm{d}x\\
&+\overline{\alpha}_2(\int_0^1\overline{Y}_2\overline{Y}_1''\int_0^1Y_1'Y_2'\mathrm{d}x\mathrm{d}x+\int_0^1\overline{Y}_2Y_1''\int_0^1\overline{Y}_1'Y_2'\mathrm{d}x\mathrm{d}x\\
&+\int_0^1\overline{Y}_2Y_2''\int_0^1Y_1'\overline{Y}_1'\mathrm{d}x\mathrm{d}x)]/(-2i\omega_2\int_0^1Y_2\overline{Y}_2\mathrm{d}x-2\beta v_0\int_0^1\overline{Y}_2Y_2'\mathrm{d}x)
\end{aligned}\tag{30}$$

If the complex amplitudes are expressed in polar form and written into the real and imaginary parts of the coefficients, the "amplitude phase modulation equations" for the uniform regime state can be simply written as,

$$\begin{aligned}\text{Re\_1} \Rightarrow\ & a_1\cos\gamma_{11}K_{11R} - a_1\sin\gamma_{11}K_{11I} \\ & + a_2(\cos\gamma_{13}\cos\gamma_{11} + \sin\gamma_{13}\sin\gamma_{11})K_{12R} \\ & + a_2(\cos\gamma_{13}\sin\gamma_{11} - \sin\gamma_{13}\cos\gamma_{11})K_{12I} \\ & - \frac{1}{4}{a_1}^2 a_2\cos\gamma_{13}K_{13R} + \frac{1}{4}{a_1}^2 a_2\sin\gamma_{13}K_{13I} \\ & + a_1K_{14R} + \frac{1}{4}{a_1}^3K_{15R} + \frac{1}{4}a_1{a_2}^2K_{16R} = 0\end{aligned} \tag{31}$$

$$\begin{aligned}\text{Im\_1} \Rightarrow\ & \frac{1}{2}a_1\sigma_2 + a_1\sin\gamma_{11}K_{11R} + a_1\cos\gamma_{11}K_{11I} \\ & + a_2(-\cos\gamma_{13}\sin\gamma_{11} + \sin\gamma_{13}\cos\gamma_{11})K_{12R} \\ & + a_2(\cos\gamma_{13}\cos\gamma_{11} + \sin\gamma_{13}\sin\gamma_{11})K_{12I} \\ & - \frac{1}{4}{a_1}^2 a_2\sin\gamma_{13}K_{13R} - \frac{1}{4}{a_1}^2 a_2\cos\gamma_{13}K_{13I} \\ & + a_1K_{14I} + \frac{1}{4}{a_1}^3K_{15I} + \frac{1}{4}a_1{a_2}^2K_{16I} = 0\end{aligned} \tag{32}$$

$$\begin{aligned}\text{Re\_2} \Rightarrow\ & -a_1(\cos\gamma_{11}\cos\gamma_{13} + \sin\gamma_{11}\sin\gamma_{13})K_{21R} \\ & - a_1(\cos\gamma_{11}\sin\gamma_{13} - \sin\gamma_{11}\cos\gamma_{13})K_{21I} \\ & + \frac{1}{4}{a_1}^3\cos\gamma_{13}K_{22R} + \frac{1}{4}{a_1}^3\sin\gamma_{13}K_{22I} \\ & + \frac{1}{4}{a_2}^3K_{23R} + a_2K_{24R} + \frac{1}{4}{a_1}^2a_2K_{25R} = 0\end{aligned} \tag{33}$$

$$\begin{aligned}\text{Im\_2} \Rightarrow\ & a_2[\frac{3}{2}\sigma_2 - \sigma_1] - a_1(-\cos\gamma_{11}\sin\gamma_{13} \\ & + \sin\gamma_{11}\cos\gamma_{13})K_{21R} - a_1(\cos\gamma_{11}\cos\gamma_{13} \\ & + \sin\gamma_{11}\sin\gamma_{13})K_{21I} - \frac{1}{4}{a_1}^3\sin\gamma_{13}K_{22R} \\ & + \frac{1}{4}{a_1}^3\cos\gamma_{13}K_{22I} + \frac{1}{4}{a_2}^3K_{23I} + a_2K_{24I} \\ & + \frac{1}{4}{a_1}^2a_2K_{25I} = 0\end{aligned} \tag{34}$$

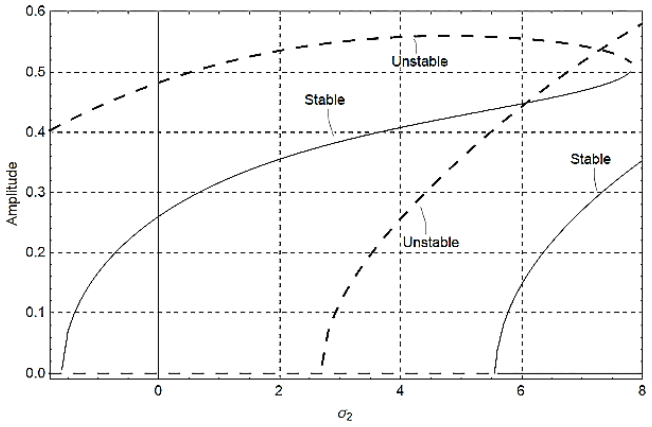

Figure 2 Change of the amplitude a_1 according to the detuning parameter σ_2 (Case 1)

By using the marked natural frequency values for cases 1 to 3 and the equations obtained for the cases where the fundamental parametric resonance due to the fluid velocity and the 3:1 internal resonance coincide, the graphs that show the variations of the amplitudes depending on the fluid velocity detuning parameter (σ_2) are plotted in Figs. 2-7.

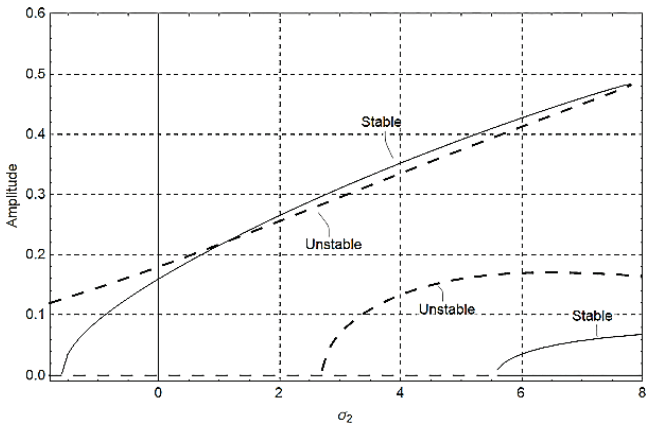

Figure 3 Change of the amplitude a_2 according to the detuning parameter σ_2 (Case 1)

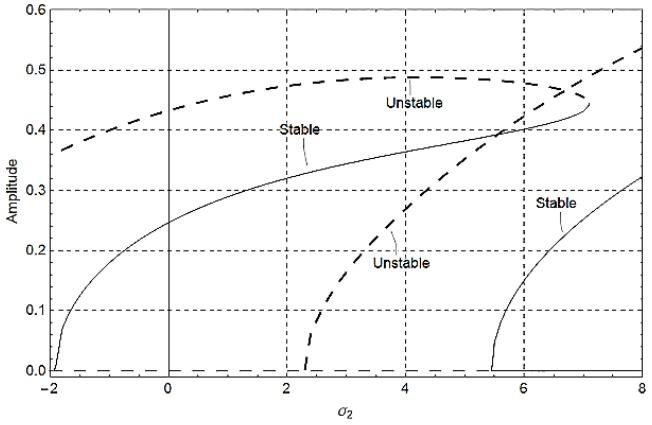

Figure 4 Change of the amplitude a_1 according to the detuning parameter σ_2 (Case 2)

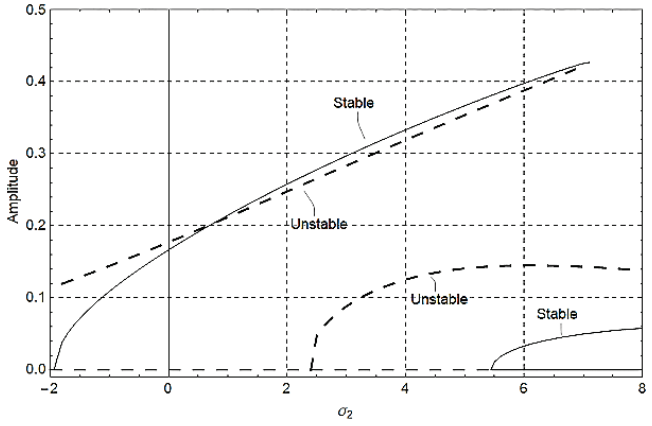

Figure 5 Change of the amplitude a_2 according to the detuning parameter σ_2 (Case 2)

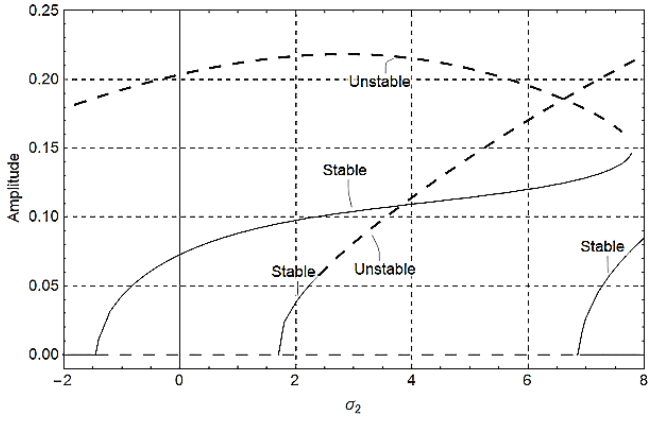

Figure 6 Change of the amplitude a_1 according to the detuning parameter σ_2 (Case 3)

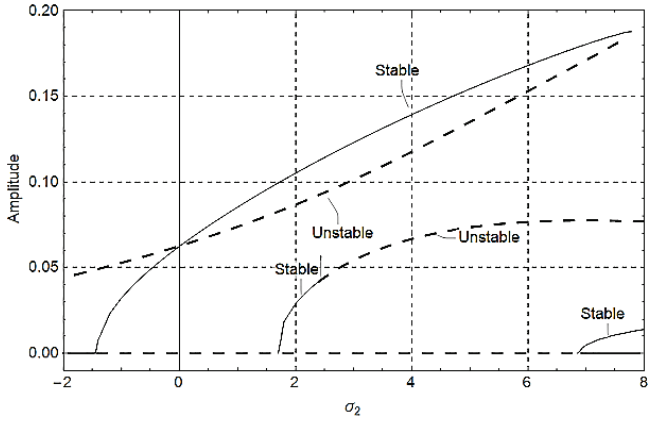

Figure 7 Change of the amplitude a_2 according to the detuning parameter σ_2 (Case 3)

In these graphs, force amplitude and damping ratio are taken as 1 ($F=1,\mu=1$). Figs. 2 and 3 show the first and second mode amplitude changes depending on the detuning parameter for case 1. Figs. 4 and 5 show the first and second mode amplitude changes depending on the detuning parameter for case 2. Figs. 6 and 7 show the first and second mode amplitude changes depending on the detuning parameter for case 3. Stable and unstable roots of the amplitudes and stability regions can be seen from these graphs. Beam coefficient is 1, 0.8 and 0.1 in these graphs respectively. When beam coefficient decreases, the amplitudes also decrease, but unstable regions become wider in detuning parameter axis.

3.2 The Case Where the Dominant Resonance and 2:1 Internal Resonance Conditions are Together

In this case, the fluid velocity change frequency is taken as the critical forcing frequency. The frequency of the electric voltage change was chosen so as not to create any secularity.

$$\begin{aligned}&\omega_2 = 2\omega_1 + \varepsilon\sigma_1\\ &2\Omega_2 = \omega_1 + \varepsilon\sigma_2\\ &\Omega_1 \not\approx 0, \omega_1, 2\omega_1\end{aligned} \tag{35}$$

When similar operations are performed in this case, amplitude phase modulation equations are obtained as follows,

$$\begin{aligned}&\mathrm{Re\_1} \Rightarrow a_1K_{11R} + \frac{1}{4}a_1{}^3K_{12R} + \frac{1}{4}a_1a_2{}^2K_{13R}\\ &+2(\cos\gamma_{11}K_{14R} - \sin\gamma_{11}K_{14I})\\ &+a_2(\cos\gamma_{12}K_{15R} - \sin\gamma_{12}K_{15I}) = 0\end{aligned} \tag{36}$$

$$\begin{aligned}&\mathrm{Im\_1} \Rightarrow a_1\sigma_2 + a_1K_{11I} + \frac{1}{4}a_1{}^3K_{12I} + \frac{1}{4}a_1a_2{}^2K_{13I}\\ &+2(\cos\gamma_{11}K_{14I} + \sin\gamma_{11}K_{14R})\\ &+a_2(\cos\gamma_{12}K_{15I} + \sin\gamma_{12}K_{15R}) = 0\end{aligned} \tag{37}$$

$$\begin{aligned}&\mathrm{Re\_2} \Rightarrow a_2K_{21R} + \frac{1}{4}a_1{}^2a_2K_{22R} + \frac{1}{4}a_1{}^2a_2K_{23R}\\ &+a_1(\cos\gamma_{12}K_{24R} + \sin\gamma_{12}K_{24I}) = 0\end{aligned} \tag{38}$$

$$\begin{aligned}&\mathrm{Im\_2} \Rightarrow -a_2\sigma_1 + a_2K_{21I} + \frac{1}{4}a_1{}^2a_2K_{22I}\\ &+\frac{1}{4}a_1{}^2a_2K_{23I} + a_1(\cos\gamma_{12}K_{24I} - \sin\gamma_{12}K_{24R}) = 0\end{aligned} \tag{39}$$

From the equations obtained for the case where the dominant resonance and 2:1 internal resonance coincide, the graphs that show the variations of the amplitudes depending on the fluid velocity detuning parameter (σ_2) are plotted as follows,

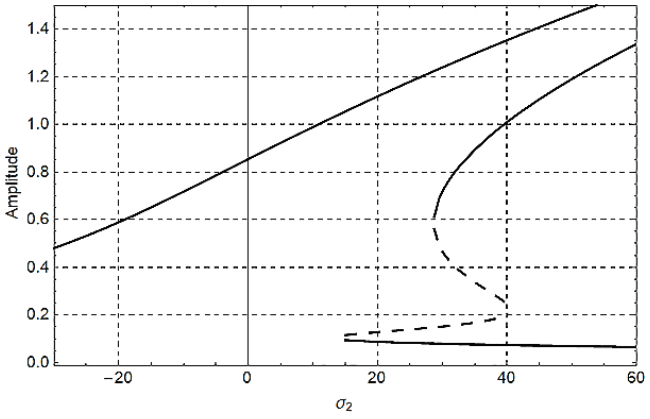

Figure 8 Change of the amplitude a_1 according to the detuning parameter σ_2 (Case 4-1)

In these graphs, force amplitude and damping ratio are both taken as 8 ($F=8,\mu=8$) for case 4-1 and force amplitude is taken as 2 and damping ratio is taken as 8 ($F=2,\mu=8$) for case 4-2. Figs. 8 and 9 show the first and second mode amplitude changes depending on the detuning parameter for case 4-1. Figs. 10 and 11 show the first and second mode amplitude changes depending on the detuning parameter for case 4-2. Stable and unstable roots of the

amplitudes and stability regions can be seen from these graphs. The stability limits become clearer as the force is decreased. In case 4-1 amplitude curves show a different structure. Dominant resonance has more effect on stability regions when force has a higher value. Structures in Figs. 8 and 9 are the combination of internal and external resonance cases. From cases 4-1 and 4-2, we can see that when force amplitude decreases, the amplitudes slightly decrease.

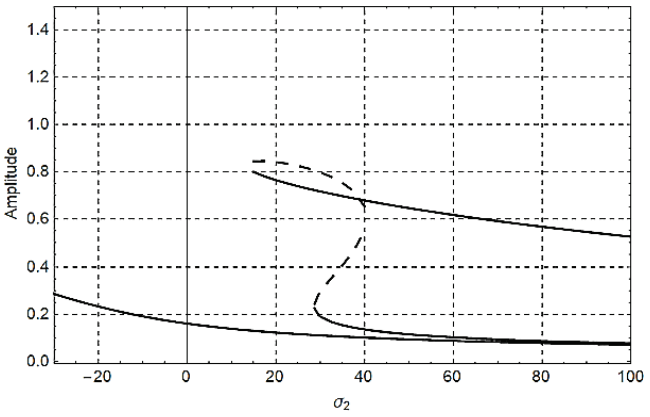

Figure 9 Change of the amplitude a_2 according to the detuning parameter σ_2 (Case 4-1)

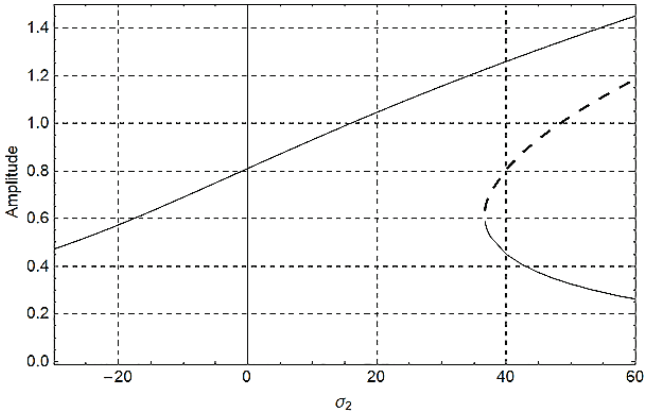

Figure 10 Change of the amplitude a_1 according to the detuning parameter σ_2 (Case 4-2)

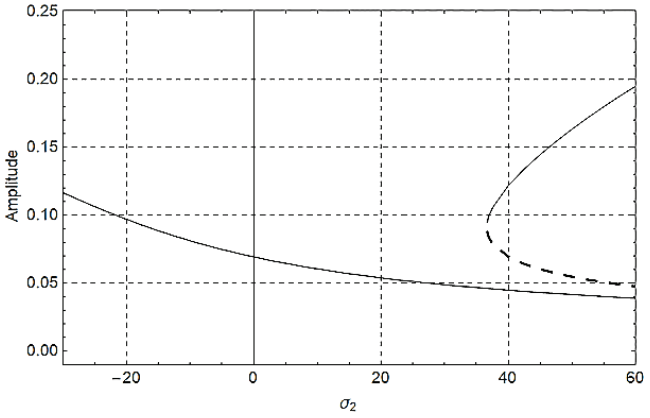

Figure 11 Change of the amplitude a_2 according to the detuning parameter σ_2 (Case 4-2)

4 CONCLUSIONS

The transverse vibrations of a microbeam conveying fluid have been investigated. The method of multiple scales and modified couple stress theory have been applied to obtain approximate solutions. First two natural frequencies and possible 3:1 and 2:1 internal resonance cases have been calculated and represented in tables. For the nonlinear problem, 3:1 and 2:1 internal resonances have been investigated. For case 1, when $v_0 = 4.550$, $\omega_1 = 22.345$ and $\omega_2 = 67.150$, for case 2, when $v_0 = 3.70$, $\omega_1 = 17.916$ and $\omega_2 = 53.790$, for case 3, when $v_0 = 1.350$, $\omega_1 = 2.437$ and $\omega_2 = 7.348$ 3:1 internal resonance case can occur. For case 4, when $v_0 = 0.500$, $\omega_1 = 4.901$ and $\omega_2 = 9.805$, 2:1 internal resonance case can occur. For these cases amplitude phase modulation equations have been obtained and by solving these equations stability borders have been drawn. At certain critical values of fluid velocity, 3: 1 or 2: 1 internal resonance states can occur. These critical fluid velocities have been evidenced in the graphs by the unstable regions that can cause significant problems in terms of system operation. The fluid velocity should not be close to the critical value so that the system can operate safely. As the beam coefficient increases, the critical velocity values at which internal resonances occur are reduced. While the critical velocity of 3:1 internal resonance is about 4.5, when the beam coefficient is 1, this value drops to about 1.35 when the beam coefficient is 0.1. Using more rigid materials will make the system safer again. But if fluid velocity is high enough for internal resonance case in rigid microbeam (Case 1), amplitudes are higher than less rigid microbeam cases.

This work can be developed in many ways:

1) Different resonance interactions such as the combination of total and difference type resonances, different internal resonances, resonances arising from interactions with more than one mode can be considered.
2) Application problems in which boundary conditions are not ideal can be considered.

ACKNOWLEDGEMENTS

This study was supported by Manisa Celal Bayar University Scientific Research Units (BAP) project number BAP-2013-130

5 REFERENCES

[1] Hassanpour, P. A., Cleghorn, W. L., Esmailzadeh, E., & Mills, J. K. (2007). Vibration analysis of micro-machined beam-type resonators. *Journal of Sound and Vibration, 308*, 287-301. https://doi.org/10.1016/j.jsv.2007.07.043

[2] Romig, Jr, A. D., Dugger, M. T., & McWhorter, P. J. (2003). Materials issues in microelectromechanical devices: science, engineering, manufacturability and reliability. *Acta Materialia, 51*, 5837-5866. https://doi.org/10.1016/S1359-6454(03)00440-3

[3] Onur Ekici, H. (2006). Mikro makinelerde kiriş titreşimlerinin analizi. *M.Sc. Thesis*, CBU. Institute of Science and Technology.

[4] Kaplan, H., & Dölen, M. (2003). Micro–Elektro–Mekanik Sistemler (MEMS): Üretim Teknikleri. *11. National Symposium on Machine Theory*.

[5] Kaplan, H., & Dölen, M. (2003). Micro–Elektro–Mekanik Sistemler (MEMS): Mikro Akışkan Uygulamaları. *11. National Symposium on Machine Theory*, Gazi University, Faculty of Engineering and Architecture, 4-6 Sept.

[6] Feynman, R. P. (1959). There's Plenty of Room at the Bottom. *American Physical Society Meeting*, Pasadena CA.

[7] Paidoussis, M. P., Grinevich, E., Adamovic, D., & Semler, C. (2002). Linear and nonlinear dynamics of cantilevered cylinders in axial flow. Part 1: Physical dynamics. *Journal of Fluids and Structures, 16*(6), 691-713. https://doi.org/10.1006/jfls.2002.0447

[8] Paidoussis, M. P., Semler, C., Wadham-Gagnon, M., & Saaid, S. (2007). Dynamics of cantilevered pipes conveying fluid. Part 2: dynamics of the system with intermediate spring support. *Journal of Fluids and Structures, 23*, 569-587. https://doi.org/10.1016/j.jfluidstructs.2006.10.009

[9] Rinaldi, S., Prabhakar, S., Vengallatore, S., & Paidoussis, M. P. (2010). Dynamics of microscale pipes containing internal fluid flow: damping, frequency shift, and stability. *Journal of Sound and Vibration, 329*, 1081-1088. https://doi.org/10.1016/j.jsv.2009.10.025

[10] Kural, S., & Özkaya, E. (2012). Vibrations of an Axially Accelerating, Multiple Supported Flexible Beam. *Structural Engineering and Mechanics, 44*, 521-538. https://doi.org/10.12989/sem.2012.44.4.521

[11] Yurddaş, A., Özkaya, E., & Boyacı, H. (2012). Nonlinear Vibrations of Axially Moving Multi-Supported Strings Having Non-Ideal Support Condition. *Nonlinear Dynamics, 73*, 1223-1244. https://doi.org/10.1007/s11071-012-0650-5

[12] Yurddaş, A., Özkaya, E., & Boyacı, H. (2012). Nonlinear Vibrations and Stability Analysis of Axially Moving Strings Having Nonideal Mid-Support Conditions. *Journal of Vibration and Control, 20*, 518-534. https://doi.org/10.1177/1077546312463760

[13] Kural, S., & Özkaya, E. (2017). Size-dependent vibrations of a micro beam conveying fluid and resting on an elastic foundation. *Journal of Vibration and Contro*l, 23(7). https://doi.org/10.1177/1077546315589666

[14] Fleck, N. A., Muller, G. M., Ashby, M. F., & Hutchinson, J. W. (1994). Strain gradient plasticity: theory and experiment. *Acta Metallurgica et Materialia, 42*, 475-487. https://doi.org/10.1016/0956-7151(94)90502-9

[15] Yang, F., Chong, A. C. M., Lam, D. C. C., & Tong, P. (2002). Couple stressbased strain gradient theory for elasticity. *International Journal of Solids and Structures, 39*, 2731-2743. https://doi.org/10.1016/S0020-7683(02)00152-X

[16] Park, S. K., & Gao, X. -L. (2006). Bernoulli–Euler beam model based on a modified couple stress theory. *Journal of Micromechanics and Microengineering, 16*, 2355-2359. https://doi.org/10.1088/0960-1317/16/11/015

[17] Kong, S. L., Zhou, S. J., Nie, Z. F., & Wang, K. (2008). The size-dependent natural frequency of Bernoulli–Euler micro-beams. *International Journal of Engineering Science, 46*, 427-437. https://doi.org/10.1016/j.ijengsci.2007.10.002

[18] Chen, W., Li, L., & Xu, M. (2011). A modified couple stress model for bending analysis of composite laminated beams with first order shear deformation. *Composite Structures, 93*, 2723-2732. https://doi.org/10.1016/j.compstruct.2011.05.032

[19] Rafiee, M., & Nezamabadi, A. (2011). Forced Oscillatıon of Simply-Supported Microbeams Considerıng Nonlinear Effects. *International Journal of Engineering & Applied Sciences (IJEAS), 3*(1), 27-41.

[20] Ke, L. -L., Wang, Y. -S., Yang, J., & Kitipornchai, S. (2012). Free vibration of size-dependent Mindlin microplates based on the Modified Couple stress theory. *Journal of Sound and Vibration, 331*, 94-106. https://doi.org/10.1016/j.jsv.2011.08.020

[21] Atcı D., & Bağdatlı S. M. (2017). Free vibrations of fluid conveying microbeams under non-ideal boundary conditions. *Steel and Composite Structures, 24*(2), 141-149.

[22] Atcı D., & Bağdatlı S. M. (2017). Vibrations of fluid conveying microbeams under non-ideal boundary conditions. *Microsystem Technologies, 23*(10), 4741-4752. https://doi.org/10.1007/s00542-016-3255-y

[23] Dai, H. L., Wu, P., & Wang, L. (2017). Nonlinear dynamic responses of electrostatically actuated microcantilevers containing internal fluid flow. *Microfluidics and Nanofluidics, 21*, 162. https://doi.org/10.1007/s10404-017-1999-z

[24] Dehrouyeh-Semnani, A. M., Nikkhah-Bahrami, M., & Yazdi, M. R. H. (2017). On nonlinear vibrations of micropipes conveying fluid. *International Journal of Engineering Science, 117*, 20-33. https://doi.org/10.1016/j.ijengsci.2017.02.006

[25] Dehrouyeh-Semnani, A. M., Nikkhah-Bahrami, M., & Yazdi, M. R. H. (2017). On nonlinear vibrations of micropipes conveying fluid. *International Journal of Engineering Science, 120*, 254-271. https://doi.org/10.1016/j.ijengsci.2017.08.004

[26] Arvin, H. (2017). The Flapwise Bending Free Vibration Analysis of Micro-rotating Timoshenko Beams Using the Differential Transform Method. *Journal of Vibration and Control*, October 17, 2017. https://doi.org/10.1177/1077546317736706

[27] Lotfi, M., Moghimi Zand, M., Hosseini, I. I., Baghani, M., & Dargazany, R. (2017). Transient behavior and dynamic pull-in instability of electrostatically-actuated fluid-conveying microbeams. *Microsyst Technol, 23*, 6015-6023. https://doi.org/10.1007/s00542-017-3503-9

[28] Kural, S. (2013). Akışkan Taşıyan Mikro Kiriş Titreşimleri. *PhD. Thesis*, CBU. Institute of Science and Technology.

Author's contact:

Saim KURAL, Assistant Professor Dr.
Mechanical Engineering Dept., Manisa Celal Bayar University
MCBU Engineering Faculty AB-18, 45140 Yunusemre-Manisa, Türkiye
+90 236 201 2380
saimkural@gmail.com